

Conformational Stability of Dimeric HIV-1 and HIV-2 Reverse Transcriptases[†]

G. Divita,^{‡,§} K. Rittinger,^{||} T. Restle,[⊥] U. Immendorfer,[‡] and R. S. Goody^{*,||}

Max-Planck-Institut für Medizinische Forschung, Abteilung Biophysik, Jahnstrasse 29, 69120 Heidelberg, Germany, Max-Planck-Institut für Molekulare Physiologie, Abteilung Physikalische Biochemie, Postfach 102664, 44026 Dortmund, Germany, and Department of Molecular Biophysics and Biochemistry, Yale University, New Haven, Connecticut 06511

Received August 1, 1995; Revised Manuscript Received October 2, 1995[®]

ABSTRACT: The dissociation of dimeric reverse transcriptase (RT) of the human immunodeficiency virus (HIV) types 1 and 2 has been investigated using acetonitrile as a dissociating agent. The equilibrium transitions were monitored by combining different approaches (fluorescence spectroscopy, polymerase activity assay, and size-exclusion HPLC). The dissociation of RT induced a complete loss of polymerase activity and a 25% increase of the intrinsic fluorescence. It is fully reversible, and the midpoints of the equilibrium transition curves are dependent on the concentration of the enzyme used, suggesting a two-state transition model for the dissociation of RT in which dimers are in equilibrium with folded monomers. For both RTs, the heterodimeric form is more stable against dissociating agents and different pH than the corresponding homodimeric form. Moreover, heterodimeric HIV-2 RT exhibits a higher stability than HIV-1 RT, with a free energy of dissociation of 12.1 kcal/mol at pH 6.5 and 25 °C, instead of 10 kcal/mol for HIV-1 RT. The binding of a primer/template induces a marked conformational change in both RTs, shown by the lower accessibility of the tryptophans to quenchers and the increase in tryptophan heterogeneity, and stabilized the dimeric form of both RTs (10–100-fold). The central role of hydrophobic interactions in dimer formation has been revealed by the 30% increase of exposure of the tryptophan cluster to quenchers upon dissociation of RT and the binding of 4 equiv of 1-anilino-8-naphthalenesulfonate to the dissociated enzymes.

The biologically relevant form of human immunodeficiency virus reverse transcriptase (HIV RT)¹ is a heterodimer containing two polypeptides of 66 and 51 kDa in HIV-1 and 68 and 54 kDa in HIV-2. The smaller subunit is derived from the larger one by proteolytic cleavage of the C-terminal domain (Di Marzo-Veronese et al., 1986; Lightfoote et al., 1986).

The determination of the three-dimensional structure of heterodimeric HIV-1 RT has been an important step for a better understanding of the structure–function relationships of this enzyme. The structure has been solved in three different states: in the absence of substrate (Rodgers et al., 1995; Esnouf et al., 1995), complexed with nonnucleoside inhibitors (Kohlstaedt et al., 1992; Ren et al., 1995; Ding et al., 1995a,b), and in a ternary complex with a double-stranded DNA template/primer and a monoclonal antibody Fab fragment (Jacobo-Molina et al., 1993), and reveals an asymmetric interaction of the two subunits. Each subunit contains four similar subdomains, called palm, finger, thumb, and connection, forming the polymerase domain and the fifth

subdomain of the p66 subunit corresponding to RNase H (Kohlstaedt et al., 1992).

Due to its essential role in the life cycle of HIV, in which it converts the single-stranded genomic RNA into double-stranded proviral DNA, RT constitutes one of the main targets for chemotherapy against HIV. An interesting feature of HIV-RT is the fact that the dimeric form of the enzyme is absolutely required for all enzymatic activities (Müller et al., 1989, 1991; Restle et al., 1990, 1992a). Recently, we have proposed that the dimerization process can be a potential target for the design of a new class of inhibitors based on peptides derived from the dimer interface (Divita et al., 1994) which is mainly dominated by hydrophobic interactions between the two connection subdomains (Nanni et al., 1993; Wang et al., 1994). The detailed investigation of the dimerization process of HIV RT has revealed a two-step process with an essential role of the central tryptophan cluster of the connection subdomain in the first stage: subunit–subunit association. The following step, an isomerization in which enzymatic activity is established, involves other subdomains of the subunits, the finger and thumb subdomains of p51 (Divita et al., 1995).

To complement the kinetic studies of RT dimerization, it is important to characterize in a thermodynamic way the parameters which control the stability of the dimeric forms of RT, in order to understand the biological structure and function of RT and to design new inhibitors. In the present work, we have investigated the conformational stability of dimeric HIV-1 and HIV-2 RT and the different parameters which control the formation of the active enzyme. The studies on the dissociation process of HIV RT were

[†] This work was supported by the Bundesministerium für Forschung und Technologie (BMFT) and the Max-Planck-Gesellschaft.

* Corresponding author.

[‡] Max-Planck-Institut für Medizinische Forschung.

[§] Present address: CRBM-CNRS, 1919 Route de Mende, BP 5051, 34033 Montpellier, France.

^{||} Max-Planck-Institut für Molekulare Physiologie.

[⊥] Yale University.

[®] Abstract published in *Advance ACS Abstracts*, December 1, 1995.

¹ Abbreviations: AIDS, acquired immunodeficiency syndrome; *E. coli*, *Escherichia coli*; HIV-1, HIV-2, human immunodeficiency virus type 1 and type 2; RT, reverse transcriptase; ANS, 1-anilino-8-naphthalenesulfonate; bis-ANS, 5,5'-bis[8-(phenylamino)-1-naphthalenesulfonate].

performed at equilibrium by combining complementary approaches, namely, intrinsic and extrinsic fluorescence spectroscopy, activity measurements, and HPLC size-exclusion. The results lead to the conclusion that the heterodimers constitute the most stable form of both RTs and that significant differences between the two enzymes exist in terms of spectroscopic properties and energetics of subunit dimerization.

EXPERIMENTAL PROCEDURES

Materials. Acetonitrile, guanidinium chloride, acrylamide, and potassium iodide were from Merck (Darmstadt, Germany), ANS and bis-ANS were purchased from Molecular Probes (Inc.), and [^3H]dTTP was obtained from Amersham.

Enzyme Preparation. Recombinant HIV-1_{BH10} and HIV-2_{D194} reverse transcriptases were expressed in *E. coli* and purified as described before (Müller et al., 1989, 1991). Highly homogeneous preparations of the heterodimeric forms of the enzyme resulting from coexpression of the 66 and 51 kDa subunits (68 and 54 kDa for HIV-2 RT, respectively) were used. Purified p66/p66 HIV-1 and p68/p68 HIV-2 homodimers were obtained as previously described (Restle et al., 1990; Müller et al., 1991). In spite of this difference in molecular masses, we have used the nomenclature of "p66" and "p51" subunits for the HIV-2 RT in analogy to the related polypeptides from HIV-1 RT. Enzyme concentrations were routinely determined according to Bradford (1976) using a gravimetrically prepared solution of RT as standard.

Oligonucleotides. Oligodeoxynucleotides were synthesized on an Applied Biosystems 380 B DNA synthesizer and purified by HPLC reverse-phase chromatography on a Hypersil C18 column (Divita et al., 1995). Primer and template oligodeoxynucleotides were annealed by heating an equimolar mixture of both in 20 mM Tris-HCl, pH 7.5, for 15 min at 70 °C, followed by cooling to room temperature over a period of 2 h in a water bath. Routinely, an 18/36-mer oligonucleotide primer/template was used with the nucleotide sequence corresponding to the sequence of the natural primer binding site (PBS) (Wain-Hobson et al., 1985).

Polymerase RT Assay. Polymerase activity was measured in a standard reaction assay using poly(rA)•(dT)₁₅ as template/primer (Restle et al., 1990). The RT preparations used showed a specific activity of about 10 000 units/mg, where 1 unit of enzyme catalyzes the incorporation of 1 nmol of [^3H]dTTP in 10 min at 37 °C into acid-insoluble material. The assays were performed on samples containing 50 ng of protein for 5 min at 37 °C. The short time was chosen to limit the possibility of further activation by association. Analyzing the effect of pH on polymerase activity, both heterodimeric HIV-1 and HIV-2 RTs were incubated for 12 h in different buffers with pH values ranging from 4.5 to 8.5. The buffers used were 50 mM Tris-HCl (pH 8.5–7) and 50 mM Mes or Mops-HCl (pH 6.5–4.5), containing 5% glycerol to increase the enzyme stability.

HPLC Size-Exclusion Chromatography. Chromatography was performed using two HPLC columns in series (Bio-Rad TSK-250 followed by Bio-Rad TSK-125; both 7.5 × 300 mm). The samples containing 5–10 µg of protein were applied and eluted with 200 mM potassium phosphate (pH 7.0) at a flow rate of 0.8 mL/min (Restle et al., 1990).

Fluorescence Experiments. Fluorescence measurements were performed at 25 °C using a SLM Smart 8000 spec-

trofluorometer equipped with a PH-PC 9635 photomultiplier, using spectral band-passes of 2 and 8 nm for excitation and emission, respectively. The intrinsic fluorescence emission of RT was measured in a total volume of 0.7 mL of fluorescence buffer containing 50 mM Tris-HCl (pH 8.0) or 50 mM Mes-HCl (pH 6.5), 10 mM MgCl₂, 50 mM KCl, 5% glycerol, and 1 mM dithiothreitol. Analyzing the effect of magnesium, the same buffer without MgCl₂ was used, and 1 mM EDTA was added to chelate Mg²⁺ traces. The enzyme was routinely excited at 290 nm, and the emission spectrum was integrated between 315 and 420 nm.

The bis-ANS fluorescence emission was integrated between 440 and 580 nm, upon excitation at 355 or 290 nm. Stock solutions of ANS and bis-ANS in TE-buffer, pH 8.0 (10 mM Tris-HCl and 1 mM EDTA), were prepared and filtered, and the concentration was checked by using extinction coefficients of 8000 M⁻¹ cm⁻¹ at 372 nm for ANS and 22 000 M⁻¹ cm⁻¹ at 394 nm for bis-ANS. For kinetic experiments, the final concentration of bis-ANS used was 5 µM, and the emission fluorescence resulting from energy transfer between Trp residues and bis-ANS was monitored at 490 nm. All measurements were corrected for the background intensity of the buffer, for the dilution effects, and for the wavelength dependence of the exciting light intensity by the use of the quantum counter Rhodamine B. The Raman scatter contribution was removed by subtracting buffer blank.

Fluorescence Quenching Experiments. Quenching titrations with either acrylamide or potassium iodide were performed at 25 °C by sequential addition of aliquots from 6–7 M stock solutions, up to 0.4 M final concentration. The potassium iodide stock solution contained 0.1 mM sodium thiosulfate to prevent I₃⁻ formation. Using NaCl, it was shown that ionic strengths up to 0.4 M did not significantly modify the fluorescence emission of both HIV-1 and HIV-2 RTs. The data were corrected for dilution (less than 5%) and for the buffer blank. The corrections for the inner filter effect due to acrylamide absorption were calculated according to Calhoun et al. (1983), and the standard experiments were performed on a solution of NATA, a tryptophan model compound. All the given values were the means of four separate experiments.

The fluorescence quenching data in the presence of either iodide or acrylamide were analyzed according to the Stern–Volmer equation, which assumes that all quenching is collisional (no static quenching) (Eftink & Ghiron, 1981):

$$F_0/F = 1 + K_{sv}[Q] \quad (1)$$

where F_0 and F are the fluorescence intensities, respectively, in the absence or the presence of the quencher, K_{sv} is the collisional Stern–Volmer constant, and $[Q]$ is the quencher concentration. The plot of F_0/F versus $[Q]$ is linear for a homogeneous population of emitting fluorophores. In contrast, fluorophore heterogeneity leads to a downward deviation from the linearity and can be calculated using the modified Stern–Volmer relationship (Lehrer, 1971):

$$F_0/(F_0 - F) = 1/[Q]f_aK_Q + 1/f_a \quad (2)$$

where f_a is the fractional number of accessible fluorophores and K_Q their collisional constant. The plot of $F_0/(F_0 - F)$ versus $1/[Q]$ allows a graphical determination of f_a .

Dissociation and Association of the Dimeric RTs under Equilibrium Conditions. Dissociation of hetero- and homodimeric HIV-1 and HIV-2 RT was achieved by addition of acetonitrile (up to 25%) in the fluorescence buffer. The dissociation was monitored under equilibrium conditions by measuring the relative change of the intrinsic fluorescence emission of the protein, the decrease of the polymerase activity, and size-exclusion HPLC (Divita et al., 1993a). All experiments were performed at 25 °C with an enzyme concentration in the range of 1–10 μM (10 μM for the homodimeric form) in a total volume of 0.7 mL of appropriate buffer containing the required concentration of acetonitrile. To analyze the reversibility of the dissociation process, heterodimeric RTs were completely dissociated by the addition of 20% acetonitrile, and subunit association was induced by a 15-fold dilution of the sample with an organic solvent free buffer [50 mM Tris-HCl (pH 8.0), 10 mM MgCl_2 , 50 mM KCl, 5% glycerol, and 1 mM dithiothreitol], resulting in a final concentration of 1.3% acetonitrile. The dissociation experiments in the presence of primer/template were performed using a concentration of 8 μM of 18/36-mer primer/template.

Dissociation Kinetics. The establishment of the dissociation equilibrium was followed in a time-dependent manner by monitoring the increase of both the intrinsic protein and bis-ANS fluorescence and the decrease of the polymerase activity of RT. Intrinsic fluorescence excitation was routinely performed at 290 nm, and the emission was measured at the wavelength of greatest intensity change (340 nm). For dissociation kinetics, a protein concentration of 2 or 10 μM was used. The data were evaluated using the program "GrafIt" (Erithacus software), which allows the user to define his own equations, and the time courses of dissociation of the hetero- and homodimer were fitted by a first-order equation with a single rate constant.

Data Analysis. Dissociation data from the fluorescence and polymerase activity measurements of the hetero- and homodimer RTs were transformed to give the relative fraction of monomers. For each value of f_{obs} , the monomeric fraction of RT (M_m) was calculated by applying the equation (Pace, 1986; Pace et al., 1990):

$$M_m = (f_{\text{obs}} - f_d)/(f_m - f_d) \quad (3)$$

where f_d and f_m are the fluorescence intensities (or the polymerase activity) of dimeric (obtained in the absence of dissociating agent) and monomeric RT (obtained at high concentration of dissociating agent), respectively.

Assuming a one-step model for the reversible dissociation of the HIV-1 and HIV-2 RT heterodimer, the process can be described by the equation:

$$K_d = [M]^2/[D] \quad (4)$$

where D represents the heterodimeric form and M the monomeric forms of RT.

The total concentration of monomers (M_t) at any concentration of acetonitrile can be defined in terms of the fraction of monomeric protein (M_m) as obtained from the fluorescence measurements, and the K_d can be expressed in terms of the measurable values M_t and M_m :

$$K_d = 2M_t(M_m)^2/(1 - M_m) \quad (5)$$

Table 1: Quenching Parameters of HIV-1 and HIV-2 Reverse Transcriptase^a

RT	acrylamide			iodide		
	K_{sv}^b (M^{-1})	K_Q^c (M^{-1})	f_a^c	K_{sv}^b (M^{-1})	K_Q^c (M^{-1})	f_a^c
HIV-1						
RT dimeric	6.0	12	0.67	2.4	4.8	0.5
RT + PT	3.7	7.6	0.5	1.6	5.4	0.34
RT monomeric	9	11	1	5.2	6	0.8
RT unfolded	14.1	15	1	8	9	1
HIV-2						
RT dimeric	5.5	9	0.75	2	4.4	0.6
RT + PT	3.0	5.2	0.5	1.4	3.8	0.35
RT monomeric ^d	8.2	10	1	4.8	6.8	0.8
RT unfolded	16.2	16	1	7	8.2	1
NATA	20	19	1	12	12	1

^a RTs (0.5 μM) were incubated at pH 8.0 (^dpH 6.5) in the presence or in the absence of 0.8 μM primer/template and mixed with increasing amounts of acrylamide or iodide up to concentrations of 0.4 M. Total unfolded RTs were obtained by overnight incubation with 6 M Gdn-HCl, and dissociation of RT was induced by treatment with 17% acetonitrile. In all cases, the excitation was performed at 290 nm and the emission recorded at 340 nm. Control experiments under the same conditions were conducted with a NATA solution instead of RT. ^b The K_{sv} constant was graphically estimated by the initial slope from the Stern–Volmer plots. ^c The fractional number of accessible fluorophores (f_a) and K_Q constants were extrapolated from the modified Stern–Volmer equation (see Experimental Procedures).

For the determination of the free energy of both heterodimeric RT dissociations, we have used the two-state denaturation model according to Pace et al. (1990) where the free energy of dissociation is defined as a linear function of the concentration of the dissociating agent acetonitrile:

$$\Delta G_d = \Delta G_d^{\text{H}_2\text{O}} + m[A] = -RT \ln K_d \quad (6)$$

where m is the slope of the plot of ΔG_d versus $[A]$. $[A]$ is the concentration of acetonitrile; R and T are the gas constant and the absolute temperature, respectively. ΔG_d was calculated via the K_d at the corresponding concentrations of acetonitrile using eq 6. $\Delta G_d^{\text{H}_2\text{O}}$ is the extrapolated free energy of dissociation in the absence of a dissociating agent.

RESULTS

Conformational Stability of HIV-1 and HIV-2 RT As Monitored by Fluorescence Quenching. Heterodimeric HIV-1 and HIV-2 RTs contain 37 and 35 tryptophan residues, respectively, which lead to high intrinsic fluorescence signals with a maximal emission centered at 338 nm (Divita et al., 1993a). This intrinsic fluorescence of RT can be used as a probe which is extremely sensitive to modifications in the microenvironment of the fluorophores. Quenching experiments with acrylamide and iodide have been used to determine the solvent exposure of the tryptophan residues and the conformational transitions of both HIV-1 and HIV-2 RTs.

As shown in Figure 1, the tryptophan residues of heterodimeric HIV-1 RT exhibit limited accessibility toward both quenchers. For the native form of HIV-1 RT, relatively low Stern–Volmer constant values (K_{sv}) of 6 and 2.4 M^{-1} were obtained for acrylamide and iodide, respectively. These values are ca. 2–4-fold lower than those obtained for NATA or the unfolded enzyme (Table 1). The Stern–Volmer plots for iodide (Figure 1A) presented a marked downward deviation from linearity, which corresponds to a significant

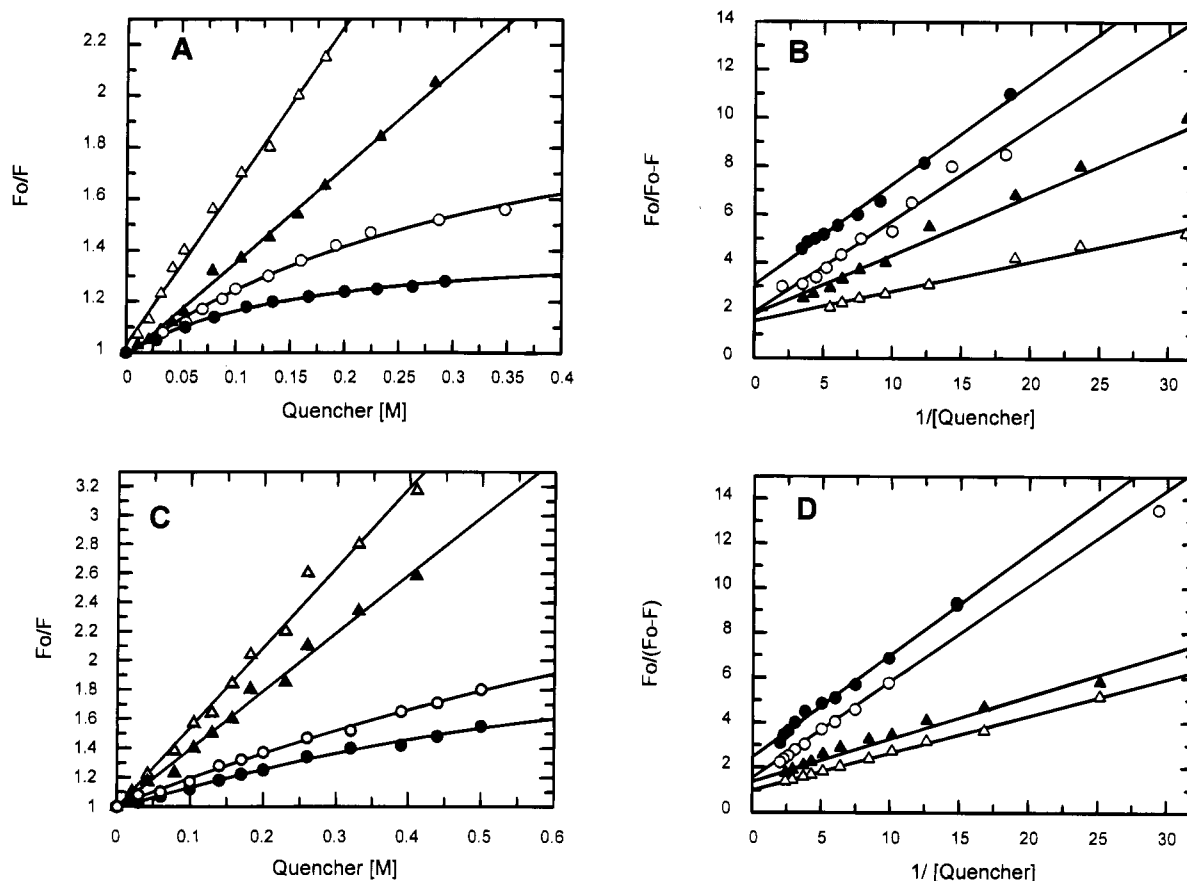


FIGURE 1: Acrylamide and iodide quenching of HIV-1 and HIV-2 RT intrinsic fluorescence. RTs (0.5 μ M) were first incubated in the presence (close symbols) or in the absence (open symbols) of P/T and then mixed with increasing amounts of acrylamide (triangles) and iodide (circles). The emission was measured at 340 nm upon excitation at 290 nm. The data were analyzed as described under Experimental Procedures, according to the Stern–Volmer equation [(A) HIV-1 RT, (C) HIV-2 RT] and to the Lehrer equation [(B) HIV-1 RT, (D) HIV-2 RT].

tryptophan heterogeneity toward this quencher. The modified Stern–Volmer plot (Figure 1B) leads to estimates of the accessible fraction (f_a) of 0.67 for acrylamide and 0.5 for iodide. The slope of the straight line allowed the calculation of an apparent K_Q constant for the accessible fraction of 12 and 4.8 M^{-1} for acrylamide and iodide, respectively. Heterodimeric HIV-2 RT presents similar quenching parameters to those of HIV-1 RT (Figure 1C,D) with a large tryptophan heterogeneity toward both quenchers (Table 1). The tryptophan residues appear to be less accessible than in the case of HIV-1 RT, with lower K_{sv} values of 5.5 M^{-1} for acrylamide and 2 M^{-1} for iodide (Table 1). For both RTs, it was shown that under the conditions used neither acrylamide nor iodide induced dissociation of the subunits.

The quenching induced by iodide was accompanied by a 12 nm blue shift of the emission spectrum from 338 to 326 nm at higher quencher concentrations (0.4 M). This large blue shift revealed the presence of different tryptophan populations in the dimeric form of both RTs, as already suggested by the relatively low f_a value for this quencher. In contrast, no shift was observed in the presence of acrylamide which induced only a decrease in the fluorescence intensity (data not shown).

Unfolding of both enzymes achieved by overnight incubation in 6 M Gdn-HCl induced a 14 nm red shift of the maximal emission from 338 to 352 nm and a 30% quenching of fluorescence intensity. Both effects reflect an increase

in the solvent exposure of the tryptophan residues, which alters their fluorescence (Bursteins et al., 1973; Pace et al., 1990). Moreover, the unfolding of RT completely abolished tryptophan heterogeneity ($f_a = 1$) and strongly increased the K_{sv} values, which became similar to the K_Q values (Table 1).

Conformational Change Induced by Primer/Template Binding. As we have already shown, the binding of a primer/template to RT results in a large quenching of the intrinsic fluorescence (Divita et al., 1993b). As described in Figure 1, the presence of saturating concentrations of a primer/template strongly reduced the exposure of the tryptophan residues to both quenchers. The Stern–Volmer constants obtained were 3.7 M^{-1} (HIV-1) and 3.0 M^{-1} (HIV-2) for acrylamide and 1.6 M^{-1} (HIV-1) and 1.4 M^{-1} (HIV-2) for iodide. Moreover, tryptophan heterogeneity was significantly increased with residual accessible fraction values of 0.5 and 0.34 for acrylamide and iodide (HIV-1 RT), respectively, which suggests that a significant conformational change of the enzyme takes place upon binding of the primer/template.

Stability of HIV-1 and HIV-2 RT as a Function of pH. The effect of the pH on the stability of both RTs was studied by monitoring the residual polymerase activity after 12 h incubation at different pH values in the range of 4.5–8.5 (Figure 2). Neither HIV-1 nor HIV-2 heterodimer RT polymerase activities were affected nor dissociation was induced after 12 h incubation at pH values between 8.5 and 7.2. In contrast, the stability of HIV-1 RT is dramatically

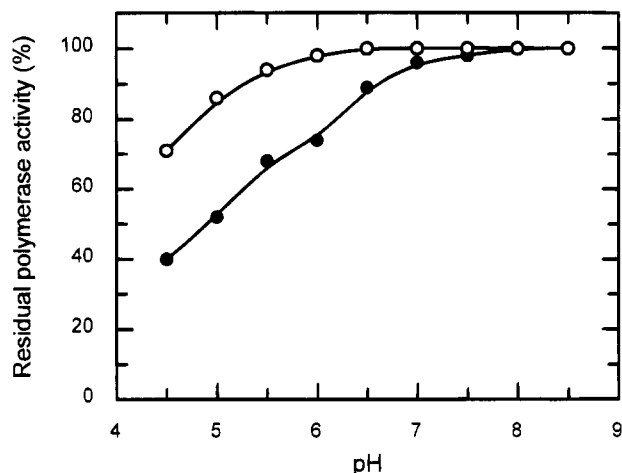


FIGURE 2: Effect of pH on the polymerase activity of HIV-1 and HIV-2 RT. HIV-1 (●) and HIV-2 (○) heterodimeric RTs (5 μ M) were incubated for 12 h at different pH values between 4.5 and 8.5. The residual polymerase activity was determined on an aliquot fraction containing 40 ng of protein using the standard method as described under Experimental Procedures.

reduced at lower pH values, and the polymerase activity decreased rapidly in a time-dependent manner (data not shown). After 12 h incubation at pH 4.5, only 40% and 70% residual polymerase activity was detected for HIV-1 and HIV-2 RT, respectively. Analyzing the RTs by size-exclusion HPLC revealed that this loss of polymerase activity is mainly due to enzyme dissociation.

In contrast to HIV-1 RT, previous studies (Müller et al., 1991a) have shown that at pH 8.0 it was not possible to reversibly dissociate heterodimeric HIV-2 RT by treatment with organic solvents, due to the high stability of this enzyme. A pH-dependent study showed that at pH 6.5 both RTs can be reversibly dissociated by the combined effects of lowering the pH and organic solvents. Working at pH 6.5 thus leads to the possibility of making a detailed comparative analysis of the stability of HIV-1 and HIV-2 RTs. After 12 h incubation at this pH, a decrease of 30% of HIV-1 RT polymerase activity was noted, whereas HIV-2 RT is quite stable for at least 12 h. Short exposure of the enzymes to pH 6.5 did not result in loss of activity.

Equilibrium Dissociation of HIV-1 and HIV-2 RTs. At pH 6.5, both heterodimeric RTs can be reversibly dissociated by acetonitrile treatment without inducing unfolding of the monomers or protein precipitation. The dissociation of HIV-1 and HIV-2 RT induced a large increase in the intrinsic fluorescence intensity (27%) and a 7 nm red shift of the emission maximum (from 338 to 345 nm). The dissociation of both RTs was attended by a significant increase of the exposure of the Trp-residues to both quenchers, with corresponding K_{sv} values of 9 and 5.2 M^{-1} for acrylamide and iodide (HIV-1 RT), respectively (Table 1). Such modifications of the fluorescence properties are characteristic of tryptophan side chains partially shielded from the aqueous solvent.

The acetonitrile-mediated dissociation of RT was also investigated by monitoring the loss of RNA-dependent DNA polymerase activity. The large modifications of the protein fluorescence and protein activity occurring upon dissociation have been used to establish the thermodynamic and kinetic parameters of subunit interaction for both heterodimeric RTs, in comparison with the corresponding homodimeric forms

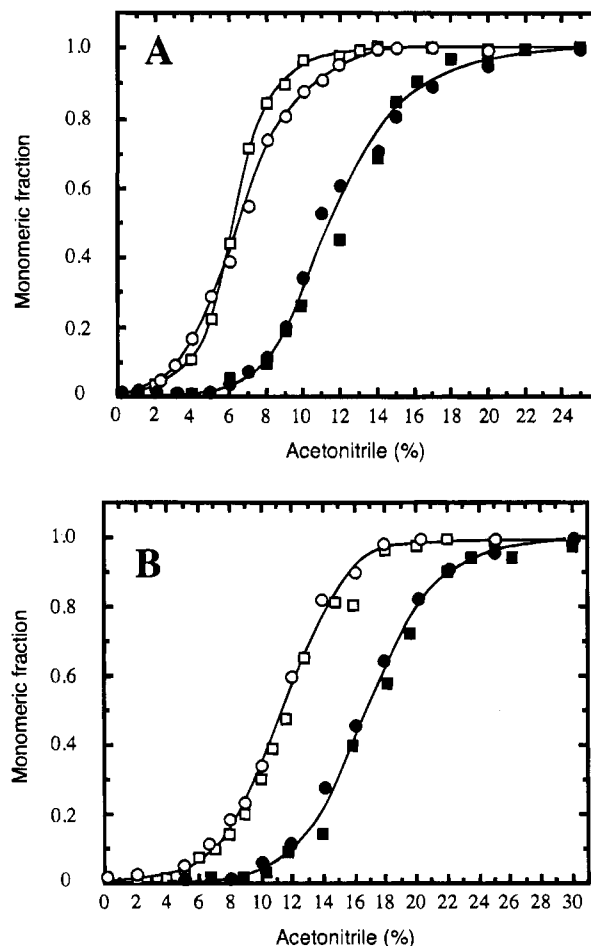


FIGURE 3: Dependence of the apparent monomeric fraction of HIV-1 and HIV-2 RT on the acetonitrile concentration. Both 5 μ M of heterodimeric HIV-1 (panel A) and 5 μ M HIV-2 (panel B) RT were incubated in the standard fluorescence buffer at pH 6.5 and 25 $^{\circ}$ C in the presence (close symbols) or in the absence (open symbols) of 5 μ M primer/template. Acetonitrile-induced dissociation of heterodimeric RT was monitored by the change in intrinsic fluorescence (circles) or by measuring the polymerase activity (squares).

(p66/p66). In all cases, the fluorescence signal was stable after 20 min incubation in the respective acetonitrile concentration, and for each acetonitrile concentration used, the amount of monomeric form was measured by size-exclusion HPLC. The data were transformed in terms of the monomeric fraction and are reported in Figure 3.

The dissociation transition curves obtained for HIV-1 and HIV-2 heterodimeric RT (5 μ M) revealed a sharp single sigmoidal transition, and complete dissociation was obtained with 12% and 18% acetonitrile, respectively (Figure 3A,B). This effect was correlated with complete monomerization, as shown by size-exclusion HPLC, agreeing well with the other approaches (Table 2). As expected, acetonitrile-induced RT dissociation is dependent on the total protein concentration used, the values of the transition midpoint ($C_{1/2}$) increasing linearly with the RT concentration in the range of 1–10 μ M (Table 2), which confirms that both RTs dissociate in a single-phase transition. Therefore, HIV-2 RT appears to be much more stable with a transition midpoint value ($C_{1/2}$) of 11.2% acetonitrile, about 2-fold higher than that obtained for HIV-1 RT (5.8%).

The dissociation transition curves obtained in the presence of saturating amounts of a primer/template (Figure 3A,B)

Table 2: Thermodynamic Parameters for the Acetonitrile-Induced Dissociation Transition of HIV-1 and HIV-2 RT^a

	HIV-1 RT			HIV-2 RT		
	$\Delta G_d^{H_2O}$ (kcal/mol)	[ACN] _{1/2} (%)	K_d (M)	$\Delta G_d^{H_2O}$ (kcal/mol)	[ACN] _{1/2} (%)	K_d (M)
Heterodimer, pH 6.5, 25 °C ^b						
RT, 5 μ M	10.2 \pm 0.6	5.8	1.3×10^{-8}	12.5 \pm 0.5	11.2	7.1×10^{-10}
+primer/template	12.3 \pm 0.4	12	2.2×10^{-10}	14.2 \pm 0.3	15	5.3×10^{-11}
RT, 10 μ M	11.4 \pm 0.5	7.2	7.8×10^{-9}	13.7 \pm 0.7	10.7	2.5×10^{-11}
Heterodimer, pH 8.0, 25 °C ^c						
none	12.3 \pm 0.5	8.7	4.05×10^{-10}	<i>d</i>		
primer/template	13.4 \pm 0.2	11.8	4.7×10^{-11}	<i>d</i>		
Homodimer (p66/p66), pH 8.0, 25 °C ^e						
	8.1 \pm 0.6	5.2	4.5×10^{-7}	8.6 \pm 0.5	6.5	1.8×10^{-7}

^a Dissociation transitions were monitored by the intrinsic fluorescence at 340 nm, upon excitation at 290 nm, and by size-exclusion HPLC. The concentrations of heterodimer and homodimer used are 5 and 10 μ M, respectively, in the respective fluorescence buffer (Experimental Procedures).

^b The values of $\Delta G_d^{H_2O}$ and [ACN]_{1/2} were derived from a two-state model analysis of the transition according to eq 6, and the K_d values were calculated using eq 5. ^c HIV-1 RT data at pH 8.0 according to Divita et al. (1993a). ^d At this pH, it is not possible to dissociate HIV-2 RT using acetonitrile. ^e At pH 6.5, the homodimeric forms of RT (p66/p66) were not stable enough for a thermodynamic study.

also give a single sharp sigmoidal transition. Complete dissociation is obtained with 20% and 26% acetonitrile with transition midpoint values of 12.0 and 15.0% acetonitrile for HIV-1 and HIV-2 RT (5 μ M), showing that the stability of the dimeric forms is strongly increased in the presence of a primer/template. Similar experiments have been performed at pH 8.0 with the corresponding HIV-1 and HIV-2 p66/p66 homodimer. In fact, with the homodimeric form of RT, it was not possible to work at pH 6.5, because at this pH the enzyme is not stable enough for a complete characterization of the dissociation process (data not shown). The dissociation curve obtained at a homodimer concentration of 10 μ M (at this concentration, less than 5% of the monomeric form is present) also reveals a sharp sigmoidal transition, and total dissociation of RT takes place for concentrations of 10% (HIV-1) and 12% (HIV-2) acetonitrile.

The reversibility of the dissociation process of both RTs was investigated using the same three methods: fluorescence spectroscopy, a polymerase activity assay, and size-exclusion HPLC. Hetero- and homodimeric RTs (5 or 10 μ M) were first dissociated by acetonitrile at pH 6.5, 25 °C (pH 8.0 for homodimer), and the solution was then diluted 15-fold into an acetonitrile-free buffer (pH 8.0). After 20 h incubation at 25 °C, a complete recovery of polymerase activity and the fluorescence properties of the dimeric form were observed, and only dimeric RT was detected by size-exclusion HPLC. The association transition curve obtained by monitoring fluorescence and size-exclusion HPLC fitted well with the dissociation curve, which is in contrast to the curve obtained by polymerase activities which reveals the presence of a second transition after dimer formation (data not shown).

Thermodynamic Parameters of HIV-1 and HIV-2 RT Dissociation. The fact that the dissociation of both RTs is dependent on the enzyme concentration used, is fully reversible, and follows a single transition curve is consistent with the notion that the acetonitrile-induced dissociation of RT occurs through a two-state model in which two populations of protein exist at equilibrium: the dimeric form (D) and folded monomers (M). Accordingly, the free energy of dissociation in the absence of acetonitrile ($\Delta G_d^{H_2O}$) can be calculated by extrapolation of the free energy to zero acetonitrile concentration (Pace et al., 1986). The thermodynamic parameters are summarized in Table 2. A $\Delta G_d^{H_2O}$

value of 12.5 kcal/mol was obtained for HIV-2 RT, as compared to 10.2 kcal/mol for HIV-1 RT, confirming the higher stability of HIV-2 RT.

The binding of primer/template strongly increased the values of $\Delta G_d^{H_2O}$ to 12.3 kcal/mol (HIV-1) and 14.2 kcal/mol (HIV-2). These results are in agreement with the high stability of the RT–primer/template complex and the marked conformational change induced by primer/template binding, as observed by fluorescence quenching experiments.

From the free energy of dissociation, the apparent equilibrium dissociation constants (K_d) for the heterodimeric forms of RT in the absence of acetonitrile (pH 6.5 and 25 °C) were calculated (Table 2). The K_d values for HIV-1 and HIV-2 heterodimeric RTs were 1.3×10^{-8} and 7.1×10^{-10} M, respectively. The presence of primer/template induced a distinct increase in the affinity of the subunits, with K_d values of 2.2×10^{-10} M (HIV-1) and 5.3×10^{-11} M (HIV-2). For the p66/p66 homodimer, the difference in the stability between HIV-1 and HIV-2 is not so significant with K_d values of 4.5×10^{-7} M (HIV-1) and 1.8×10^{-7} M (HIV-2) at pH 8.0.

Dissociation Kinetics of HIV-1 and HIV-2 RT. Dissociation of HIV-RT can be followed by monitoring the increase in the intrinsic fluorescence, which offers the possibility of studying this process in a time-dependent manner with a resolution of a few seconds. The dissociation of RT (5 μ M) was performed by adding 20% acetonitrile to the fluorescence buffer (pH 6.5 or 8.0 in the case of p66/p66 homodimer). The time curves obtained are monophasic and can be fitted as a single-exponential reaction (Figure 4). The degree of dissociation was checked by size-exclusion HPLC and a RNA-dependent DNA polymerase activity assay, and the two independent approaches revealed that full dissociation takes place under the chosen conditions. The dissociation of heterodimeric HIV-1 RT is ca. 5-fold faster than that of HIV-2 (pH 6.5, 25 °C) with k_{diss} values of 2.2×10^{-2} and 4.2×10^{-3} s⁻¹, respectively, at 20% acetonitrile (Figure 4A,B). This difference in the rate of dissociation may be directly correlated with the low thermodynamic stability of HIV-1 RT in contrast to HIV-2 RT. At pH 6.5, the k_{diss} of HIV-1 RT is 5.5-fold faster than that previously observed at pH 8.0 (Divita et al., 1993a) and fits well with the pH dependence of the dimer stability. Magnesium also plays a role in the stability of RT heterodimer, the dissociation rate constant of HIV-2 RT being increased by a factor of 2 on

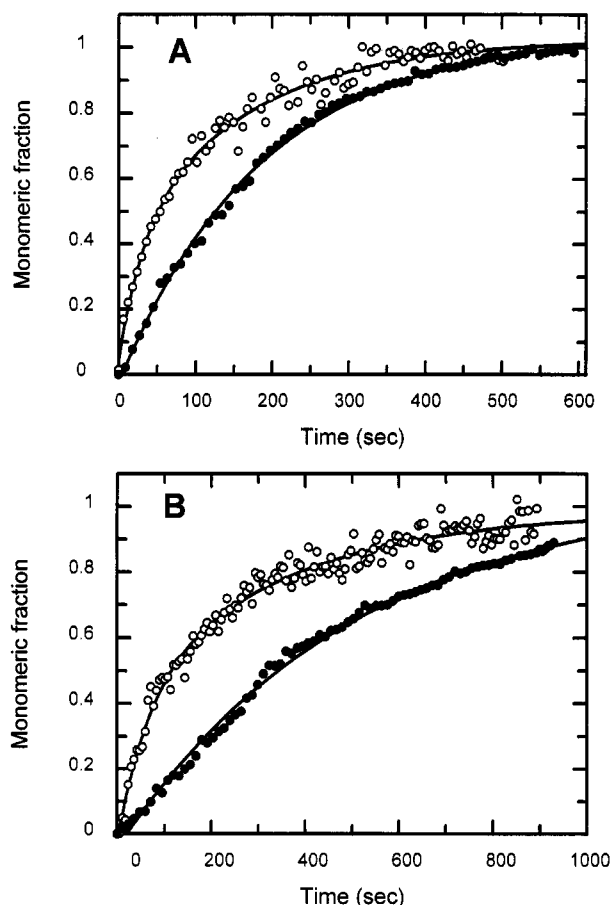


FIGURE 4: Kinetics of HIV-1 and HIV-2 RT dissociation induced by acetonitrile. HIV-1 RT (panel A) and HIV-2 RT (panel B) ($5 \mu\text{M}$) were fully dissociated by adding 20% acetonitrile, in the absence (O) or in the presence of $5 \mu\text{M}$ primer/template (●) at pH 6.5, 25°C . The kinetics of dissociation were monitored by using the increase of intrinsic fluorescence at 340 nm (excitation at 290 nm). The curves were fitted according to a first-order reaction. The fraction of monomer was calculated according to Pace et al. (1990) using eq 3 as described under Experimental Procedures.

Table 3: Kinetic Parameters for Dissociation of Homodimeric and Heterodimeric HIV RTs^a

buffer	HIV-1		HIV-2	
	p66/p66 k_{diss} (s^{-1})	p66/p51 k_{diss} (s^{-1})	p66/p66 k_{diss} (s^{-1})	p66/p51 k_{diss} (s^{-1})
pH 6.5	c	2.2×10^{-2}	c	4.2×10^{-3}
pH 6.5 + P/T	c	7.1×10^{-3}	c	1.1×10^{-4}
pH 8.0	7.2×10^{-2}	4.5×10^{-3} (8.7×10^{-3}) ^b	3.7×10^{-2}	c
pH 8.0 + P/T	1.9×10^{-2}	2.0×10^{-3} (4.2×10^{-3}) ^b	9.6×10^{-3}	c

^a Dissociation kinetics were performed by adding 20% acetonitrile to a homodimeric ($10 \mu\text{M}$) or heterodimeric ($5 \mu\text{M}$) HIV-1 and HIV-2 RT solution. The large increase of the intrinsic fluorescence upon dissociation was monitored at 340 nm (excitation at 290 nm). The curves were fitted as a single-exponential reaction. ^b The change in ANS fluorescence during RT dissociation was followed by monitoring the fluorescence energy transfer at 490 nm upon tryptophan excitation at 290 nm. ^c Homodimeric RT (p66/p66) was not stable enough at pH 6.5, and it was not possible to reversibly dissociate HIV-2 RT at pH 8.0 using acetonitrile treatment.

removal of magnesium, whereas HIV-1 RT was not stable enough at this pH to follow the kinetics in the absence of magnesium (Table 3). The binding of primer/template to the RTs reduced the dissociation rate constants 4-fold to $1.1 \times 10^{-3} \text{ s}^{-1}$ (HIV-2) and 3-fold to $7.1 \times 10^{-3} \text{ s}^{-1}$ (HIV-1).

The dissociation kinetics of homodimeric RTs were also investigated by monitoring the increase in the intrinsic fluorescence (22%) in a time-dependent manner (Figure 4C). At pH 6.5 and 25°C , the homodimers were not stable enough to observe the dissociation kinetics. The dissociation was performed at pH 8.0 and 25°C , and the dissociation rate constant values obtained for the two enzymes were $7.2 \times 10^{-2} \text{ s}^{-1}$ (HIV-1) and $3.7 \times 10^{-2} \text{ s}^{-1}$ (HIV-2). At this pH, the dissociation rate for the HIV-1 homodimer (p66/p66) is 16-fold faster than for the corresponding heterodimer (Table 3).

RT Dissociation As Monitored by Extrinsic ANS and Bis-ANS Fluorescence. The binding of bis-ANS or ANS to a protein results in a large increase of its fluorescence, which is due to noncovalent interactions with hydrophobic clusters at the surface of the protein (Ptitsyn, 1994). The change in ANS fluorescence was used to monitor the variation in the exposure of the hydrophobic cluster of RT during the dissociation process. Bis-ANS binds strongly to dissociated RT, which results in a 15-fold increase of the fluorescence and a large blue shift of the emission maximum of 45 nm (from 535 to 495 nm). In contrast, in the presence of fully dimeric RT, the bis-ANS fluorescence was increased only 1.5-fold, and also no significant change in the fluorescence of the probe was observed with unfolded RT (overnight incubation in 6 M Gdn-HCl). The binding of bis-ANS can be monitored by following either the increase in bis-ANS fluorescence or the quenching in the intrinsic fluorescence of RT (Figure 5A). Moreover, the large overlap between the excitation spectrum of the probe and the emission spectrum of RT offers the possibility of monitoring the binding by fluorescence resonance energy transfer experiments (not shown here). The three methods lead to similar results, with an apparent K_d value of $2.1 \mu\text{M}$ and saturation reached for a concentration of the probe of $8 \mu\text{M}$ at $2 \mu\text{M}$ RTs, which suggests a ratio of 4 mol of probe/mol of RT.

The characteristic change in the fluorescence of bis-ANS upon binding to dissociated RT is a useful signal for monitoring the kinetics of dissociation. Heterodimeric HIV-1 RT ($5 \mu\text{M}$) was first incubated in the presence of $8 \mu\text{M}$ bis-ANS, and the dissociation was then started by addition of 20% acetonitrile. The time dependence of the change in fluorescence was measured by following the fluorescence energy transfer (Figure 5B). An initial rapid 3-fold increase of fluorescence was observed during the dead time of the experiment, which is not associated with dissociation of the dimer. The increase in ANS fluorescence follows a single-exponential reaction with a rate constant of $8.7 \times 10^{-3} \text{ s}^{-1}$ which is 2-fold lower in the presence of primer/template and quite similar to the value obtained by monitoring the intrinsic fluorescence (Table 3).

DISCUSSION

We have recently described peptides whose sequence is derived from the connection subdomain of RT and which, *in vitro*, are quite powerful inhibitors of RT dimerization (Divita et al., 1994). In order to provide a basis for designing more powerful inhibitors which can disrupt the dimeric form of RT, we have now investigated the conformation and the stability of the homo- and heterodimeric forms of HIV-1 and HIV-2 RT in detail. The thermodynamic and kinetic characterization of the dissociation process of both RTs was

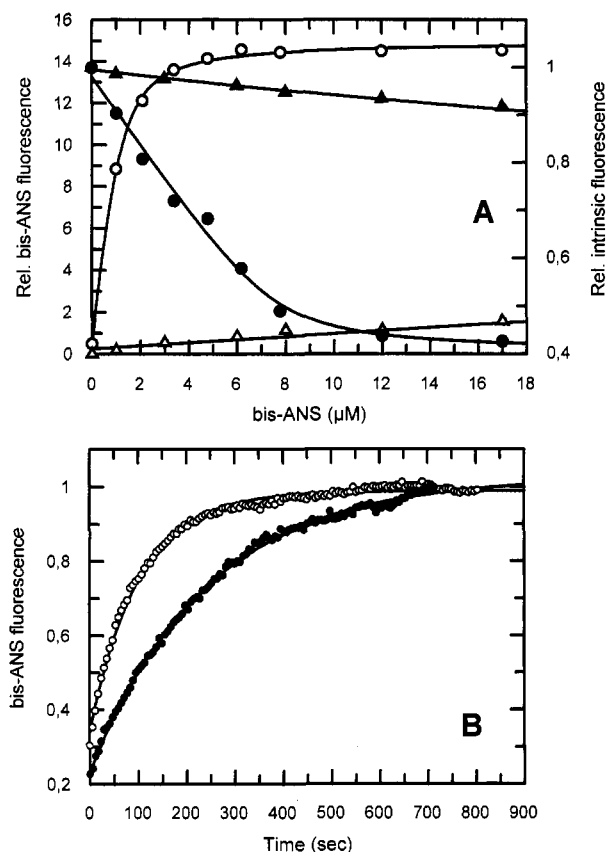


FIGURE 5: Binding of bis-ANS to HIV-1 RT. Panel A: Native heterodimeric (triangles) and dissociated (circles) HIV-1 RTs (2 μM) were incubated in the presence of increasing concentrations of bis-ANS. The binding of bis-ANS was monitored either by the increase of its extrinsic fluorescence at 490 nm upon excitation at 290 nm (open symbols) or by the quenching of the intrinsic fluorescence of RT at 340 nm upon excitation at 290 nm (closed symbols). The data were fitted according to a quadratic equation. Panel B: Kinetics of HIV-1 RT dissociation as monitored by the binding of bis-ANS. RT (5 μM) was fully dissociated in the presence of 8 μM bis-ANS, by adding 20% acetonitrile, in the absence (○) or in the presence of 5 μM primer/template (●) at pH 6.5, 25 °C. The kinetics of dissociation were monitored by following the increase of bis-ANS fluorescence at 490 nm (excitation at 290 nm) due to the binding of the probe to the dissociated monomers, and the curves were fitted according to a first-order reaction.

performed using acetonitrile as the dissociating agent, since this treatment leads only to the formation of folded monomers. The equilibrium transitions of dissociation were monitored by combining different complementary approaches, such as fluorescence spectroscopy, size-exclusion HPLC, and an RNA-dependent DNA polymerase activity assay.

Marked Conformational Change of RT upon Binding of a Primer/Template. HIV-1 and HIV-2 heterodimeric RTs show an intrinsic fluorescence characteristic of tryptophan residues relatively buried inside the protein (emission maximum at 338 nm) with a low accessibility toward external quenchers such as iodide ($K_{\text{sv}} = 2.4 \text{ M}^{-1}$) or acrylamide ($K_{\text{sv}} = 6.0 \text{ M}^{-1}$). The presence of highly buried tryptophan residues in the dimeric RTs is also supported by the observation of a large tryptophan heterogeneity (Eftink & Ghiron, 1981), with only 50% and 70% of the fluorophores accessible to iodide and acrylamide, and by the marked blue shift (12 nm) of the emission spectrum upon iodide quenching. All the results suggest a limited accessibility to the

solvent and a compactness of the dimeric forms of RT (Burstein et al., 1973), in accordance with the X-ray structure of HIV-1 heterodimeric RT (Wang et al., 1994).

The binding of a primer/template to RT reduced the accessibility of the tryptophan residues to the quenchers (2-fold) and the fraction of fluorophores accessible to iodide (from 0.5 to 0.35) and to acrylamide (from 0.67 to 0.5). The marked increase in the compactness of RT and the large quenching of protein fluorescence (25%) observed upon primer/template binding (Divita et al., 1993a) can be interpreted in two ways, which are not necessarily mutually exclusive. Either the tryptophan residues are directly located in the primer/template binding site or the conformational change occurring upon primer/template binding alters indirectly the environment of some fluorophores. Based on the recent X-ray structure of HIV-1 RT obtained in the absence (Rodgers et al., 1995; Esnouf et al., 1995) or in the presence of a primer/template or a nonnucleoside inhibitor (Kohlstaedt et al., 1992; Jacobo-Molina et al., 1993; Ding et al., 1995a,b; Ren et al., 1995), it seems possible that both effects contribute to the large quenching in intrinsic fluorescence upon primer/template binding. The kinetics of primer/template interaction with RT have been interpreted as a two-step process: the binding of the primer/template, followed by a conformational change of the intermediate complex (Divita et al., 1993b; Rittinger et al., 1995). This conformational change upon primer/template binding has been suggested to correspond to a movement of the thumb subdomain of p66 (Patel et al., 1995). This subdomain is close to the finger subdomain of p66 in the structure obtained in the absence of substrate or a nonnucleoside inhibitor (Rodgers et al., 1995; Esnouf et al., 1995).

Structural Reorganization Induced by Dimerization of the Monomers. In the case of a dimeric protein, it is important to discriminate the contribution to the protein stability due to the tertiary structure and that of intermolecular interactions. Since the use of urea or Gdn-HCl is likely to affect both of these, it is highly likely that problems will arise in trying to distinguish the effects for a detailed study of the transition between the folded dimer and the folded monomer (Jaenicke, 1987; Neet & Timm, 1994). In order to avoid this problem, we have used acetonitrile to dissociate RT, which generates stable folded monomers, without inducing denaturation (Restle et al., 1990; Divita et al., 1993a). This approach was very helpful for analyzing the reversible dissociation of both RTs and for quantifying the free energy of interaction between the subunits. It was shown earlier that the dimerization kinetics of monomers generated from heterodimers in this manner were similar to those seen using individually prepared p66 and p51 monomers without acetonitrile treatment, suggesting that this procedure did not result in significant denaturation of the monomers, at least with the short exposure times used.

The location of a large number of tryptophan residues at the dimer interface makes protein fluorescence a sensitive tool for investigating the disruption of homo- and heterodimeric RT. Fluorescence quenching experiments are useful, since the diffusion of quenchers in the protein can be directly correlated with the folding state of the protein (Eftink, 1991, 1994). The acetonitrile-induced dissociation of RT results in a 25% increase of the intrinsic fluorescence and a red shift of the emission spectrum (7 nm). As expected, the disruption of the subunit interactions strongly

increased the solvent exposure as revealed by the dramatic increase of the accessibility to quenchers (40%) and the accessible fraction of the fluorophores to acrylamide ($f_a = 1$) and to iodide ($f_a = 0.8$).

Bis-ANS fluorescence can be used as a tool for monitoring the variation in the solvent accessibility of hydrophobic clusters of a protein and for describing the intermediate states in the protein folding pathway (Ptitsyn, 1994). The large increase in the fluorescence of bis-ANS (15-fold) upon dissociation of RT, due to the binding of 4 mol of probe/mol of dissociated RT, fits well with a large increase in the solvent exposure of the hydrophobic surface of the monomer during dissociation. These results are in perfect agreement with the presence of a "hydrophobic core" at the RT interface, as we (Restle et al., 1990; Divita et al., 1993a, 1995) and other authors (Beccera et al., 1991; Nanni et al., 1993; Wang et al., 1994) have already proposed and shown.

In contrast to the dissociation transition, the complete unfolding of both RTs by overnight incubation in the presence of 6 M Gdn-HCl induced a 30% decrease in the intrinsic fluorescence and a marked increase of the quenching parameters (Table 1). A preliminary model of the dissociation and unfolding of RT in the presence of increasing concentrations of Gdn-HCl involves three states, namely, native dimers, native monomers, and unfolded monomers. The formation of folded monomers results in an increase of the intrinsic fluorescence which is in perfect agreement with the presence of folded monomers after acetonitrile treatment (Divita, Rittinger, and Goody, unpublished results).

The results of the quenching experiments suggest the presence of at least three different tryptophan populations in the dimeric forms of RT. The marked modification of the intrinsic fluorescence properties observed upon dissociation of RT leads to the conclusion that a large number of the tryptophan residues are directly involved in the dimer interface or formation. The tryptophan cluster located in the α -helix L and β -strand 20 in the connection subdomains seems to be essential in the first stage of homodimer as well as heterodimer formation (Restle et al., 1992b; Divita et al., 1994, 1995). The strong binding of bis-ANS to the dissociated form of RT confirms the hydrophobic character of the monomer-monomer interface, which fits well with the structure-based calculations of the solvent accessibility (Wang et al., 1994) and the high salt stability of RT (Restle et al., 1990; Beccera et al., 1991). The second class of tryptophans are directly or indirectly involved in the primer/template binding site. One of this class, Trp-229, has been located close to the DNA binding cleft by using fluorescently labeled primer/template (Jacobo-Molina et al., 1993; Divita et al., 1995). The third class of tryptophans is less well-defined and probably contains residues well exposed to the solvent.

The Heterodimer Constitutes the Most Stable Conformation of HIV RT. In the present work, a detailed investigation of the dissociation of HIV-1 and HIV-2 heterodimeric RT has been performed in comparison with the corresponding homodimeric forms (p66/p66). In order to obtain comparable results between the two heterodimeric RTs, we have performed the dissociation measurements at pH 6.5, where the heterodimeric HIV-2 RT can be reversibly dissociated by acetonitrile treatment without denaturation or protein precipitation. Dissociation of HIV-1 RT at pH 8.0 was previously described in terms of a two-state model, in which

the dimeric form, D, is in equilibrium with the folded monomers, N (Divita et al., 1993a). The equilibrium dissociation transition curves obtained for the homo- or heterodimeric RT of HIV-1 and HIV-2 also followed a reversible single-step transition dependent on the dimer concentration. Analyzing the fluorescence and HPLC data according to a two-state model for the dissociation (Pace et al., 1990) allows the determination of the thermodynamic parameters in the absence of acetonitrile. This analysis shows significant differences between the two heterodimeric RTs (Table 2). At pH 6.5, 25 °C, in the presence of Mg^{2+} both heterodimeric RTs are still thermodynamically quite stable, with $\Delta G_d^{H_2O}$ values of 10.2 kcal/mol (HIV-1) and 12.5 kcal/mol (HIV-2). These values are compatible with the theoretical value for the free energy of dimerization calculated to be 20–30 kcal/mol (Wang et al., 1994). The dissociation constants of $1.3 \times 10^{-8} M^{-1}$ for HIV-1 and $7.1 \times 10^{-10} M^{-1}$ for HIV-2 are consistent with our values previously obtained at pH 8.0 but higher than the values obtained by analytical sedimentation (Beccera et al., 1991) in the absence of magnesium and at low temperature (5 °C). The differences can be partially explained by the fact that the temperature (Divita et al., 1995) and the presence of $MgCl_2$ (Divita et al., 1993a) are two critical factors for the dimerization process. In contrast, our results are in complete contradiction with the surprising observation that RT is mainly monomeric at physiological temperature (37 °C) reported by Lebowitz et al. (1994).

The 10-fold lower stability of HIV-1 RT at pH 6.5 is reflected by the acetonitrile-induced dissociation rate, which is 5-fold faster in comparison to the values obtained at pH 8.0 (Divita et al., 1993a). Moreover, the p66/p66 form of HIV-1 RT is not stable below pH 8.0. As observed at pH 8.0, the binding of the primer/template strongly favors dimer formation, with a $\Delta\Delta G^{H_2O}$ value of 2 kcal/mol, close to the value obtained at pH 8.0 for HIV-1 RT (1.5 kcal/mol).

The homodimeric form (p66/p66) of both RTs is less stable than the corresponding heterodimer, the difference in the free energy of dissociation between the two forms being about 4 kcal/mol. The dissociation constant values are in the range of 0.1 μM for both HIV-1 and HIV-2 p66/p66, which is in the same range as the values previously found in the absence of Mg^{2+} (Restle et al., 1990; Müller et al., 1991). In the case of homodimeric RT, the difference between the HIV-1 and HIV-2 enzymes is not so marked as that observed for the heterodimeric form, which is consistent with the idea that the higher stability of HIV-2 RT is mainly due to a conformational change which occurs after the cleavage of one of the RNase H domains and involves the thumb domain of the p51 subunit. These results are also supported by the fact that the rate of monomer association is similar for HIV-1 and HIV-2 heterodimeric RT, but the following maturation step is faster for HIV-2 RT (Divita et al., 1995). The low stability of the p66/p66 homodimer could be due to the energy required for maintaining the asymmetric form and unfolding one of the RNase domains, as support by structural (Jacobo-Molina et al., 1993; Wang et al., 1994) and biochemical data (Sharma et al., 1994) and by structural mapping of the protein interface using monoclonal antibodies (Restle et al., 1992b).

The acetonitrile-induced dissociation kinetics can be directly followed by intrinsic fluorescence. The kinetics are always monophasic, which fits well with a one-step model

for the disruption of the dimeric forms of RT. Therefore, the fast increase in ANS fluorescence (25%) during the first seconds of the dissociation kinetics and the difference in the transition between loss and the recovery of polymerase activity reveal the presence of a predissociation conformational change of RT. These results fit well with the fact that dimerization of RT takes place in at least two steps: first, association of the monomers followed by a slow isomerization step to form the "mature" heterodimeric form of RT, as we have recently proposed (Divita et al., 1995).

A detailed knowledge of the parameters which control the stability as well as the maturation of the HIV-1 and HIV-2 dimer RTs presents important information for the design of new inhibitors of the dimerization process. For example, the identification of a second step in the dimerization process offers a future point at which prevention of production of mature protein could be achieved.

REFERENCES

- Becerra, S. P., Kumar, A., Lewis, M. S., Widen, S. G., Abbotts, J., Karawya, E. M., Hughes, S. H., Shiloach, J., & Wilson, S. H. (1991) *Biochemistry* 30, 11707–11719.
- Bradford, M. (1976) *Anal. Biochem.* 72, 248–254.
- Burstein, A. E., Vedenkina, N. S., & Ivkova, M. N. (1973) *Photochem. Photobiol.* 18, 263–279.
- Calhoun, D. B., Vanderkooi, J. M., & Englander, S. V. (1983) *Biochemistry* 22, 1533–1539.
- Di Marzo Veronese, F., Copeland, T. D., De Vico, A. L., Rahman, R., Oroszlan, S., Gallo, R. C., & Sarngadharan, M. G. (1986) *Science* 231, 1289–1291.
- Ding, J., Das, K., Tantillo, C., Zhang, W., Clark, A. D., Jr., Jessen, S., Lu, X., Hsiou, Y., Jacobo-Molina, A., Andries, K., Pauwels, R., Moereels, H., Koymans, L., Janssen, P. A. J., Smith, R. H., Jr., Koepke, M. J., Michejda, C. J., Hughes, S. H., & Arnold, E. (1995a) *Structure* 3, 365–379.
- Ding, J., Das, K., Moereels, H., Koymans, L., Andries, K., Janssen, P. A. J., Hughes, S. H., & Arnold, E. (1995b) *Nat. Struct. Biol.* 2, 407–415.
- Divita, G., Restle, T., & Goody, R. S. (1993a) *FEBS Lett.* 324, 153–158.
- Divita, G., Müller, B., Immendorfer, U., Gautel, M., Rittinger, K., Restle, T., & Goody, R. S. (1993b) *Biochemistry* 32, 7966–7971.
- Divita, G., Restle, T., Goody, R. S., Chermann, J.-C., & Baillon, J. G. (1994) *J. Biol. Chem.* 269, 13080–13083.
- Divita, G., Rittinger, K., Geourjon, C., Deléage, G., & Goody, R. S. (1995) *J. Mol. Biol.* 245, 508–521.
- Eftink, M. R. (1991) *Methods Biochem. Anal.* 35, 127–205.
- Eftink, M. R. (1994) *Biophys. J.* 66, 482–501.
- Eftink, M. R., & Ghiron, C. A. (1981) *Anal. Biochem.* 114, 199–227.
- Esnouf, R., Ren, J., Ross, C., Jones, Y., Stammers, D., & Stuart, D. (1995) *Nat. Struct. Biol.* 2, 303–308.
- Jacobo-Molina, A., Ding, J., Nanni, R. G., Clark, A. D., Jr., Lu, X., Tantillo, C., Williams, R. L., Kamer, G., Ferris, A. L., Clark, P., Hizi, A., Hughes, S. H., & Arnold, E. (1993) *Proc. Natl. Acad. Sci. U.S.A.* 90, 6320–6324.
- Jaenicke, R. (1987) *Prog. Biophys. Mol. Biol.* 49, 117–237.
- Jaenicke, R., & Rudolph, R. (1986) *Methods Enzymol.* 131, 218–250.
- Janin, J., & Chothia, C. (1990) *J. Biol. Chem.* 265, 16027–16030.
- Kohlstaedt, L. A., Wang, J., Friedman, J. M., Rice, P. A., & Steitz, T. A. (1992) *Science* 256, 1783–1790.
- Lebowitz, J., Kar, S., Braswell, E., McPherson, S., & Richard, D. L. (1994) *Protein Sci.* 3, 1374–1382.
- Lehrer, S. S. (1971) *Biochemistry* 10, 3254–3262.
- Lightfoote, M. M., Coligan, J. E., Folks, T. M., Faucy, A. S., Martin, M. A., & Venkatesan, S. (1986) *J. Virol.* 60, 771–775.
- Lowe, D. M., Aitken, A., Bradley, C., Darby, G. K., Larder, B. A., Powell, K. L., Purifoy, J. M., Tisdale, M., & Stammers, D. K. (1988) *Biochemistry* 27, 1433–1436.
- Müller, B., Restle, T., Weiss, S., Gautel, M., Sczakiel, G., & Goody, R. S. (1989) *J. Biol. Chem.* 264, 13975–13978.
- Müller, B., Restle, T., Kühnel, H., & Goody, R. S. (1991) *J. Biol. Chem.* 266, 14709–14713.
- Nanni, R. G., Ding, J., Jacobo-Molina, A., Hughes, S. H., & Arnold, E. (1993) *Perspect. Drug Discovery Des.* 1, 129–150.
- Neet, K. E., & Timm, D. E. (1994) *Protein Sci.* 3, 2167–2174.
- Pace, C. N. (1986) *Methods Enzymol.* 131, 266–280.
- Pace, C. N., Shirley, B. A., & Thomson, J. A. (1990) in *Protein Structure: A Practical Approach* (Creighton, T. E., Ed.) pp 311–330, IRL Press, Oxford, England.
- Patel, P. H., Jacobo-Molina, A., Ding, J., Tantillo, C., Clark, A. D., Jr., Raag, R., Nanni, R. G., Hughes, S. H., & Arnold, E. (1995) *Biochemistry* 34, 5351–5363.
- Ptitsyn, O. B. (1994) *Protein Eng.* 7, 593–596.
- Ren, J., Esnouf, R., Garman, E., Somers, D., Ross, C., Kirby, I., Keeling, J., Darby, G., Jones, Y., Stuart, D., & Stammers, D. (1995) *Nat. Struct. Biol.* 2, 293–302.
- Restle, T., Müller, B., & Goody, R. S. (1990) *J. Biol. Chem.* 265, 8986–8988.
- Restle, T., Müller, B., & Goody, R. S. (1992a) *FEBS Lett.* 300, 97–100.
- Restle, T., Pawlita, M., Sczakiel, G., Müller, B., & Goody, R. S. (1992b) *J. Biol. Chem.* 267, 14654–14661.
- Rittinger, K., Divita, G., & Goody, R. S. (1995) *Proc. Natl. Acad. Sci. U.S.A.* 92, 8046–8049.
- Rodgers, D. W., Gamblin, S. J., Harris, B. A., Ray, S., Culp, J. S., Hellmig, B., Woolf, D. J., Debouck, C., & Harrison, S. C. (1995) *Proc. Natl. Acad. Sci. U.S.A.* 92, 1222–1226.
- Sharma, S. K., Fan, N., & Evans, D. B. (1994) *FEBS Lett.* 343, 125–130.
- Wain-Hobson, S., Sonigo, P., Danos, O., Cole, S., & Alizon, M. (1985) *Cell* 40, 9–17.
- Wang, J., Smerdon, S. J., Jäger, J., Kohlstaedt, L. A., Rice, P. A., Friedman, J. M., & Steitz, T. A. (1994) *Proc. Natl. Acad. Sci. U.S.A.* 91, 7242–7246.

BI9517796